OPEN

Correspondence and
requests for materials
should be addressed to
J.S.T.I. (jtsi@st-
andrews.ac.uk)

Remarkable transition from rocksalt/perovskite layered structure to fluorite/rocksalt layered structure in rapidly cooled Ln_2CuO_4

Chami N. K. Patabendige[1], Abul K. Azad[1], Paul A. Connor[1], Aurélie Rolle[2] & John T. S. Irvine[1]

[1]School of Chemistry, University of St Andrews, St Andrews, Fife, KY16 9ST, UK, [2]Univ Lille Nord de France, F-59000 Lille, FRANCE; CNRS UMR8181, Unité de Catalyse et Chimie du Solide - UCCS; ENSCL, F-59652 Villeneuve d'Ascq.

Lanthanide cuprates of formula Ln_2CuO_4 exist in two principal forms, T and T′ which are renowned for their exhibition at low temperatures of hole and electronic types of superconductivity, respectively. These structures differ primarily in the arrangement of oxygen between the perovskite layers and also in nature of the copper oxygen planes. The Cu-O distance in the T structure ($\sim$1.90 Å) is much shorter than the T′ (1.97Å), reflecting a transition between partial Cu^+ and partial Cu^{3+} character. In seeking to find compositions that bridge these two structure/electron carrier types, we observed the transition from a T structure to a T′ type structure, resulting in the metastable form T″ with slightly larger volume but similar character to T′. This transition from T to T″ is associated with 5% increase in a and a 5% decrease in c parameters of the tetragonal unit cells, which results in disintegration of ceramic bodies.

C uprate compounds have been the subject of considerable attention as superconducting materials. Bednorz and Müller[1] first discovered high-Tc superconductivity with Tc $\approx$ 30 K in $La_{2-x}Ba_xCuO_4$, and since then Tc of these materials has risen with the discovery of new oxide materials. For an example $Pb_2Sr_2(Ca,Y)Cu_3O_8$ (Tc $\approx$ 70 K)[3], $YBa_2Cu_3O_7$ (Tc $\approx$ 90 K)[4], and $Bi_2Sr_2Ca_2Cu_3O_{10}$[5]/,$Tl_2Ba_2Sr_2Ca_2Cu_3O_{10}$[6] (where Tc = 110–120 K). In these superconductors the charge carriers are holes (p-type); however, the carriers may also be electrons, (n-type), as discovered by Tokura et al.[2] for the compound with the formula of $Ln_{2-x}Ce_xCuO_4$ where the Ln is Pr, Nd, Sm and Eu. Therefore cuprates with general formula, Ln_2CuO_4 (214) can be either hole or electron superconductors, depending upon doping strategy. Electron doping can be achieved for the $Nd_{2-x}M_xCuO_4$ system (T′ phase) by substituting a tetravalent cation (Ce^{4+}, Th^{4+}, Pr^{4+}) for Nd^{3+} or by substituting a monovalent anion (F^-) for O^{2-}[2], decreasing the formal valence of Cu. Hole doping can be achieved for the La_2CuO_4 (T/O phase) by partial replacement of the La^{3+} by an alkaline metal, an alkaline earth metal or by the insertion of interstitial oxygen, fluorine or chlorine to the system thereby increasing the formal valence of the copper[7–10].

La_2CuO_4 and Nd_2CuO_4 are particularly well known as the parent phases of the p- and n-type cuprate super-conductor families with T and T′ structures, respectively. Whilst these phases have similar composition and symmetry, metal coordination and apparent Cu oxidation states are very different. Ideal Cu co-ordinations for T′ and T are 4 and 6, respectively. These copper coordinations play an important role in the choice of possible dopants and their properties.

In La_2CuO_4 (T phase) the $La_2O_2^{2+}$ layers have a rock salt structure, with La having a total oxygen coordination number of 9 and places oxygen atoms in the apical positions above and below Cu in the CuO_2^{2-} sheets. This results in a tetragonally distorted octahedral Cu-O coordination. At lower temperatures the T structure is slightly distorted from K_2NiF_4 structure and is orthorhombic. It is normally denoted as orthorhombic T phase (T/O). In Nd_2CuO_4 (T′ phase), flat CuO_2^{2-} layers, with Cu in a strictly square planar coordination alternate with $Nd_2O_2^{2+}$ layers. The $Nd_2O_2^{2+}$ layers have the fluorite structure, with Nd having a total oxygen coordination number 8 and therefore it places the oxygen atoms in this layer well away from the Cu apical position. Some researchers have explored the Nd_2CuO_4-La_2CuO_4 system, but the reported phase relationships in these systems is not consistent and depends strongly on the synthetic route, firing temperature and the stability/metastability fields of the closely related phases[11–16].
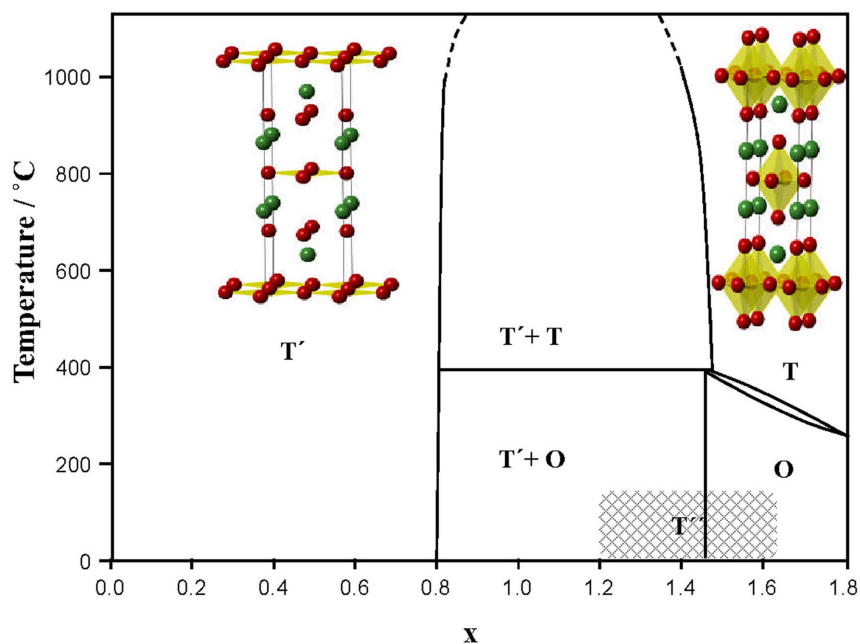
Figure 1 | Phase diagram of $Nd_{1.8-x}La_xPr_{0.2}CuO_4$ showing location of metastable T″ phase formed on rapid cooling at 950°C. Black lines show equilibrium phase boundaries. The metastable region where T″ is found on rapid cooling is shown as a hatched zone. Two inserts are schematic diagrams of T′ and T phases (green colour denotes La, Nd and Pr atoms, red colour denotes O atoms and yellow colour denotes Cu atoms).
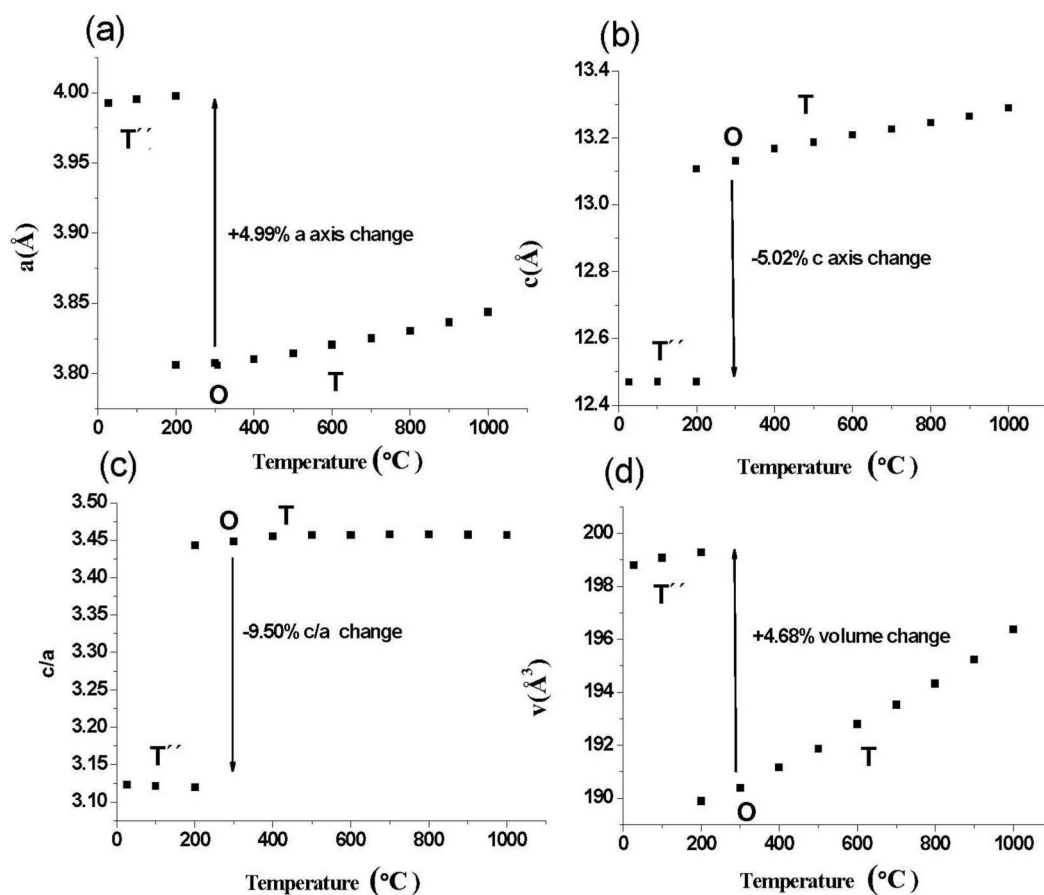

Figure 2 | Variation of lattice parameters with temperature for $Nd_{0.35}La_{1.45}Pr_{0.2}CuO_4$ (a) lattice parameter a, (b) lattice parameter c, (c) c/a ratio and (d) volume v. ESD is smaller than the symbol size for all measured points.
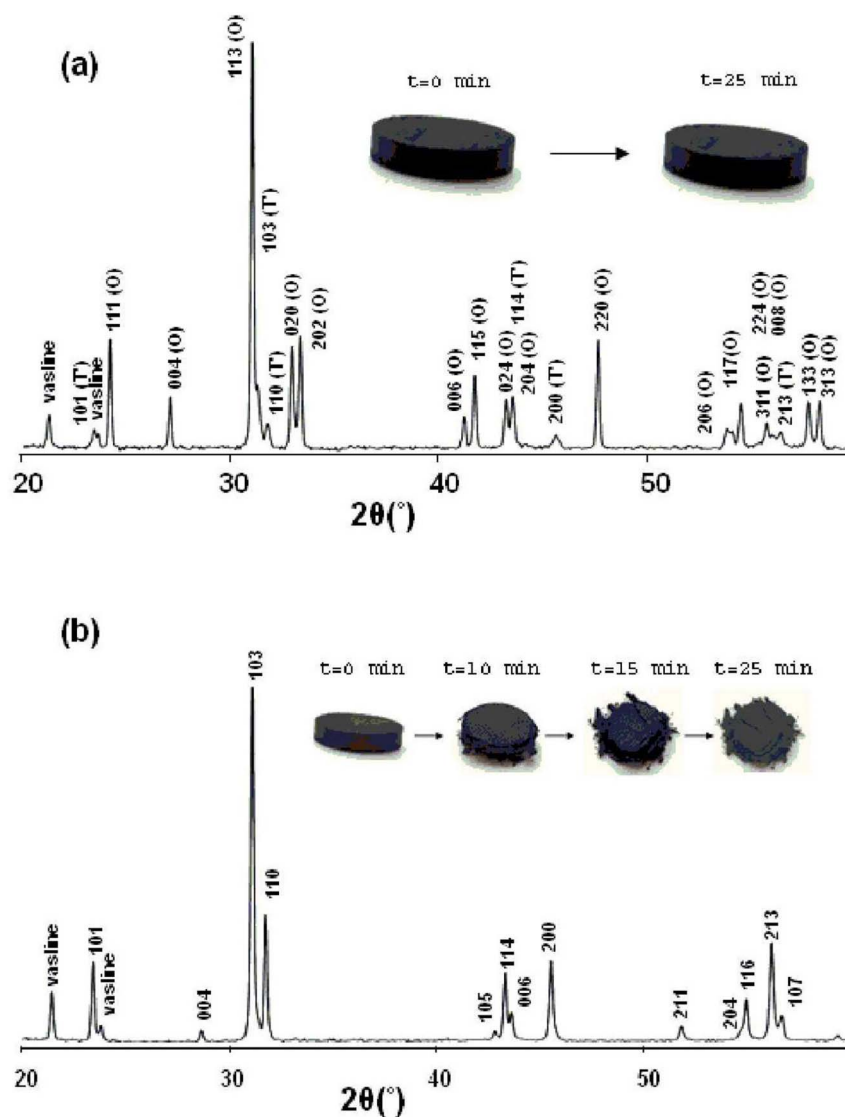
Figure 3 | 850°C and 950°C annealed pellets (with the composition $Nd_{0.35}La_{1.45}Pr_{0.2}CuO_4$) were monitored with the time after taking from the furnace and corresponding XRD patterns were collected after 2 hours for both specimens; (a) 850°C annealed pellet changes with time and corresponding room temperature XRD pattern (equilibrium spinoidal products (T′ and O phases) were observed) (b) 950°C annealed pellet changes with time and corresponding room temperature XRD pattern (T″ phase was observed).

Apart from T′ and T phases, another phase called T″ has been reported for the Nd_2CuO_4-La_2CuO_4 system where x ≈ 1.5 in $Nd_{2-x}La_xCuO_{4\pm\delta}$ which has a similar X-ray diffraction pattern to T′ with slightly larger a and c parameters. It has been suggested that T″ contains a unique cation ordering which is roughly 3(Ln):1(Ln′) in Ln-O layer and interlayer ordering at the $Ln_3Ln′$ composition and it has been defined as an equilibrium phase[11–13]. Hypotheses and suggestions on this T″ phase in literature vary and therefore we have explored this system in detail with temperature dependent X-ray diffraction, SAED, neutron diffraction and conductivity measurements.

Results

The $Nd_{1.8-x}La_xPr_{0.2}CuO_4$ system was studied varying the La substitution ratio (0 ≤ x ≤ 1.8) and then characterised using high temperature X-ray powder diffraction (Fig. S1-S3). As shown in the equilibrium phase diagram for $Nd_{1.8-x}La_xPr_{0.2}CuO_4$, Fig. 1, at room temperature, the T′ phase was found to be stable for the 0 ≤ x < 0.8 range. The orthorhombic structure (i.e. T/O) is found only between 1.45 < x ≤ 1.8. This T/O phase coexists with the T′ phase for 0.8 ≤ x

< 1.4. Above 400°C the orthorhombic T/O transforms to its tetragonal T variant. An additional metastable phase T″ may be observed especially for compositions near 1.4 < x < 1.5 when samples have been heated to higher temperatures. XRD patterns of these phases (T′, T″ and O) are compared in Fig. S4. Observance of T″ is strongly dependent upon firing temperature. In order to form this T″ phase, compositions which are within the two phase domain have to be fired above 900°C where the T phase becomes stable for compositions with x < 1.45. The metastable T″ phase is not an equilibrium phase, on annealing any rapidly cooled sample containing T″ at lower temperature, the equilibrium spinodal product phases (T′ and T/O) will be formed.

T″ phase formation was explored for the composition $Nd_{0.35}La_{1.45}Pr_{0.2}CuO_4$. XRD data were obtained on cooling from 1000°C. The T phase exists as a single phase at high temperature then transforms to metastable T″ phase at low temperatures (ca 200°C). These in situ X-ray diffraction studies indicate that T″ phase forms via the orthorhombically distorted variant (O) of the T-phase (Fig. S3). T″ has tetragonal symmetry similar to the well-known T′ type structure (Fig. S4), it has slightly larger a and c axes and c/a ratio compared
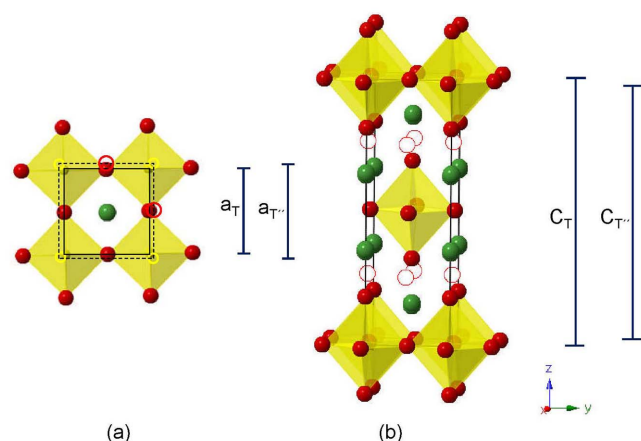
Figure 4 | Schematic diagram for T to T″ phase transformation (a) Cu-O plane top view (b) Ln-O layer view along the c direction (green colour denotes La, Nd and Pr atoms, red colour denotes O atoms and yellow colour denotes Cu atoms. Filled atoms show the T phase while the hollow atoms show the T″ phase).

to T′. This final transition is accompanied by a large change in unit cell shape, as indicated by the large difference in c/a between T and T″ phases (Fig. 2). On changing from T-type to T″-type volume increases by ∼5%, **a** increases by ∼5%, **c** decreases by ∼5% and **c/a** ratio decreases by ∼10%. As shown in Fig. 3, ceramic pellets going through the T-> T″ transition transform to fine powders within 25 minutes of cooling to room temperature. In fact, the sintered ceramic pellet of the T/O phase transforms into a fine powder (∼5 microns) of T″ (Fig. S5). After prolonged annealing of a ceramic sample at slightly lower temperature (e.g. 850°C) the T″ phase does not appear on cooling as the T phase undergoes a spinodal decomposition into higher and lower Nd content T′ and T/O phases and hence pellets remain intact after cooling to room temperature.

The T″ phase forms on relatively fast cooling, which does not allow the necessary diffusion of ions and the compositional adjustment required for the low temperature equilibrium phases to form. Therefore high temperature T phase undergoes a diffusionless transition to the metastable T″ phase. This is reminiscent of the metastable t′ phase often reported in the yttria stabilized zirconia system[17], which depends on the grain size, cooling rate and content of the Y_2O_3[18].

The T″ phase has only been obtained on cooling from 1000°C in a very narrow region where $1.4 < x < 1.5$ for this $Nd_{1.8-x}La_x$ $Pr_{0.2}CuO_4$ system. For higher La contents, the T phase is stabilised to room temperature (as its orthorhombically distorted variant). For lower La content the T′ phase is stabilised to room temperature. The observed T″ phase must have a lower free energy than the corresponding T phase, but the T″ phase is still metastable at room temperature. The symmetry of the two phases T and T′ are similar; both can be represented by the space group I4/mmm. The structure of the T″ phase has been investigated by neutron powder diffraction (Fig. S6) and it shows the typical patterns for the 4 coordinated Cu tetragonal I4/mmm phase which has larger a and c axis compared to the T′ phase. From the neutron diffraction studies, oxygen deficiency is calculated ($\delta = 0.03$). Selected area electron diffraction (Fig. S7) studies indicate that T″ has no specific cation ordering.

A schematic diagram for T to T″ phase transformation is shown in Fig. 4 with Cu-O plane top view (4a) and the Ln-O layer view (4b). The rapid transformation from T to T″ is associated with a displacement of the oxygen atom in the c direction, with a corresponding change in lattice parameters. When it changes from T to T″ Cu coordination changes from 6 to 4. As shown in Fig. 4b, octahedral

oxygen will move well away from the apical position, leading to formation of fluorite type layers in Ln-O layers.

The oxygen content of the T″ phase was also determined by thermogravimetric analysis (TGA) (Fig. S8). There is no significant mass change in the TGA under air, as the oxygen content doesn't change significantly from T to T″ phase. In order to calculate the δ values thermogravimetric analysis under 5% Hydrogen/95% Argon heating up to 1000°C were carried out. TGA indicate that reduction goes via mainly two steps. Copper reduced via Cu(I) to Cu(0). Final XRD diffraction studies also confirmed that Cu(II) was reduced to metallic copper. $\delta \approx 0.03$ ($Nd_{0.35}La_{1.45}Pr_{0.2}CuO_{3.97}$) was obtained from the measured mass loss which agrees with neutron diffraction studies.

In-situ conductivity measurements were carried out for this composition above 200°C . It shows that this composition follows metallic behaviour at higher temperatures with semiconductor metallic transition at 360°C (Fig. S9). At high temperature, this composition shows a p-type conductivity dependence increasing with oxygen partial pressure. The highest conductivity (19.7 Scm⁻¹) is reached around 360°C and this behaviour is similar to the undoped p-type T phase (La_2CuO_4), with the maximum seeming related to the T/O transition. Ceramic pellets going through T to T″ transition transform to fine powder around 200°C.

Discussion

Although $Nd_{0.35}La_{1.45}Pr_{0.2}CuO_{3.97}$ has a high Nd content, which would tend to stabilise T′ formation, it exists as a pure T phase at high temperature. This then transforms to the metastable T″ phase upon cooling if spinodal decomposition is avoided by cooling rapidly. This final transition is accompanied by a large change in unit cell parameters, resulting from the large difference in c/a ratio between T and T″ phases. The T″ phase has tetragonal symmetry and is very similar to the T′ type structure. This final transition is accompanied by a large change in unit cell parameters, as indicated by the large difference in c/a between T and T″ phases.

Methods

The T″ phase was synthesised for the $Nd_{0.35}La_{1.45}Pr_{0.2}CuO_{4\pm\delta}$ composition by solid state reaction and phase relationship was obtained using in-situ X-ray diffraction patterns. Nineteen samples with different compositions were examined to construct the phase diagram of $Nd_{1.8-x}La_xPr_{0.2}CuO_4$ family. Materials have been produced, with varying La content over the range x = 0 to x = 1.8 with an increment of 0.1, by the solid state method.

Hygroscopic powders (Nd_2O_3, Pr_6O_{11}, La_2O_3) were dried for 30 minutes at temperature up to 900°C. Stoichiometric amounts of Nd_2O_3 (Alfa-Aesar 99.9%), Pr_6O_{11} (Alfa-Aesar 99.9%), CuO (Aldrich 99+ %) and La_2O_3 (Aldrich 99.99%) were then weighed and ground in acetone. These mixtures were then dried and calcined in air at 850°C for 36 hours. Following this, powders were reground using the planetary ball mill and the heat treatment (850°C for 36 hours) repeated. Then the samples were reheated at 950°C for 24 hours.

In-situ X-ray diffraction analysis of powders were collected at room temperature on a Bruker axs D8 Advance diffractometer equipped with a solX energy dispersive detector in the 10–90° range with a step of 0.02° and a counting time of 25 s per step (CuKα = 1.5406 Å). The high temperature diffraction data were collected in the 10–90° range, with a step of 0.0148° and a counting time of 0.2 s per step, on a Bruker axs D8 Advance diffractometer equipped with a high temperature Anton Paar HTK 1200N chamber and a one dimensional X-ray detector VÅNTEC-1 (CuKα = 1.5406 Å).

The experimental procedure for sample preparation for the phase diagram and T″ phase characterisation is presented in more detail in the supplementary file.

1. Bednorz, J. B. & Müller, K. A. Possible high T_c superconductivity in Ba-La-Cu-O system. *Z. Phys. B.* **64**, 189–193 (1986).
2. Tokura, Y., Takagi, H. & Uchida, S. A superconducting copper-oxide compound with electrons as the charge-carriers. *Nature.* **337** (6205), 345–347 (1989).
3. Cava, R. J. *et al.* Superconductivity near 70-k in a new family of layered copper oxides. *Nature.* **336** (6196), 211–214 (1988).
4. Wu, M. K. *et al.* Superconductivity at 93-k in a new mixed-phase Y-Ba-Cu-O compound system at ambient pressure. *Phys. Rev. Lett.* **58** (9), 908–910 (1987).
5. Maeda, H., Tanaka, Y., Fukutomi, M. & Asano, T. A new high-Tc oxide superconductor without a rare-earth element. *Jpn. J. Appl. Phys. Part 2 - Lett.* **27** (2), L209–L210 (1988).

6. Sheng, Z. Z. & Hermann, A. M. Bulk superconductivity at 120-k in the Tl-Ca Ba-Cu-O system. *Nature.* **332** (6160), 138–139 (1988).
7. Tarascon, J. M., Greene, L. H., McKinnon, W. R., Hull, G. W. & Geballe, T. H. Superconductivity at 40-k in the oxygen-defect perovskites $La_{2-x}Sr_xCuO_{4-y}$. *Science.* **235** (4794), 1373–1376 (1987).
8. Terrance, J. B. *et al.* Properties that change as superconductivity disappears at high-doping concentrations in $La_{2-x}Sr_xCuO_4$. *Phys. Rev. B.* **40** (13), 8872–8877 (1989).
9. Axe, J. D. *et al.* Structural phase-transformations and superconductivity in $La_{2-x}Ba_xCuO_4$. *Phys. Rev. Lett.* **62** (23), 2751–2754 (1989).
10. Subramanian, M. A. *et al.* Superconducting and magnetic-behavior in $La_{2-x}Na_xCuO_4$. *Science.* **240** (4851), 495–497 (1988).
11. Goodenough, J. B. & Manthiram, A. Crystal-chemistry and superconductivity of the copper oxides. *J. Solid State Chem.* **88** (1), 115–139 (1990).
12. Manthiram, A. & Goodenough, J. B. thermal-expansion mismatch and intergrowth types in the system $La_{2-Y}Nd_YCuO_4$. *J. Solid State Chem.* **92** (1), 231–236 (1991).
13. Manthiram, A. & Goodenough, J. B. Crystal-chemistry of the $La_{2-y}Ln_yCuO_4$ (ln = pr, nd) systems. *J. Solid State Chem.* **87** (2), 402–407 (1990).
14. Ikeda, Y., Yamada, K., Kusano, Y. & Takada, J. A new tetragonal phase in La-rich $Pr_{2-x}La_xCuO_4$ (1.35 < x 1.5). *Physica C.* **378**, 395–398 (2002).
15. Singh, K. K., Ganguly, P. & Rao, C. N. R. Structural transitions in $(La,Ln)_2CuO_4$ and $La_2(Cu,Ni)O_4$ systems. *Mater. Res. Bull.* **17** (4), 493–500 (1982).
16. Wang, E., Tarascon, J. M., Greene, L. H., Hull, G. W. & McKinnon, W. R. Cationic substitution and role of oxygen in the n-type superconducting T′ system $Nd_{2-y}Ce_yCuO_z$. *Phys. Rev. B.* **41** (10), 6582–6590(1990).
17. Gibson, I. R. & Irvine, J. T. S. Qualitative X-ray diffraction analysis of metastable tetragonal (T′) zirconia. *J. Am. Ceram. Soc.* **84** (3), 615–618 (2001).
18. Scott, H. G. Phase relationships in zirconia-yttria system. *J. Mater. Sci.* **10** (9), 1527–1535 (1975).

Acknowledgements

Author contributions

C.N.K.P. and J.T.S. Irvine conceived and designed the experiments and wrote the manuscript. C.N.K.P. synthesised the material. A.K.A. participated in analysis of the results. P.C. and A.R. helped to perform high temperature XRD measurements

Additional information

How to cite this article: Patabendige, C.N.K., Azad, A.K., Connor, P.A., Rolle, A. & Irvine, J.T.S. Remarkable transition from rocksalt/perovskite layered structure to fluorite/rocksalt layered structure in rapidly cooled Ln_2CuO_4. *Sci. Rep.* **3**, 1504; DOI:10.1038/srep01504 (2013).